

Computational design of a molecular triple photoswitch for wavelength-selective control

Chong Yang^{a)}, Shavdar Slavov,^{b)} Hermann A. Wegner,^{c)} Josef Wachtveitl^{b)} and Andreas
Dreuw^{a)*}

*a) Interdisciplinary Center for Scientific Computing, Heidelberg University, Im
Neuenheimer Feld 205A, 69120 Heidelberg, Germany*

*b) Institute for Physical and Theoretical Chemistry, Goethe University, Max-von-Laue Str.
7, 60438 Frankfurt am Main, Germany*

*c) Institute of Organic Chemistry, Justus-Liebig University Giessen, Heinrich-Buff-Ring 17, 35392
Giessen, Germany*

Supporting Information

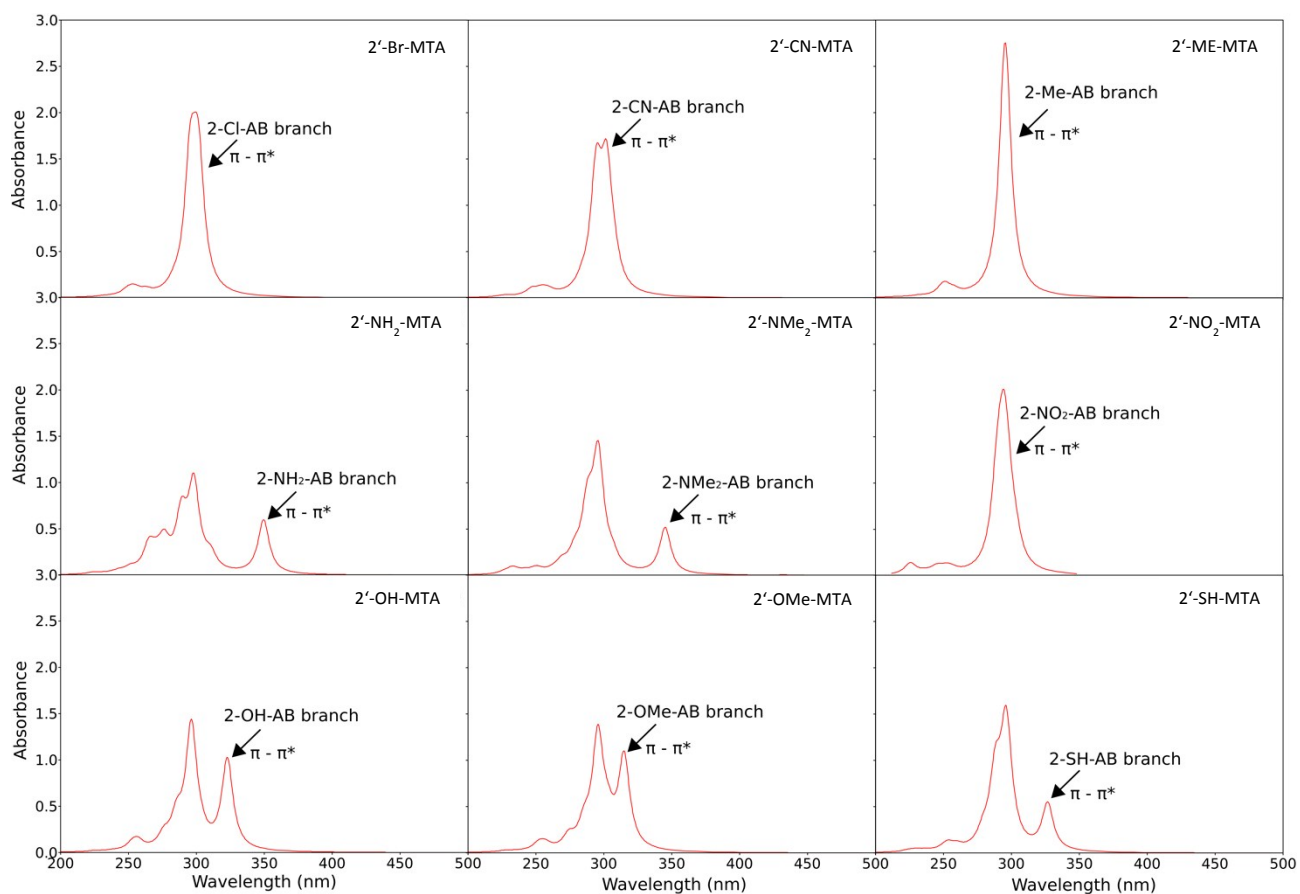


Figure S1: Simulated absorption spectra of single-branch substituted MTAs, which are all substituted at the 2' position, at the theoretical level of TDDFT/CAM-B3LYP. For the simulation of the spectra a full-width-at-half maximum of 10 nm has been used.

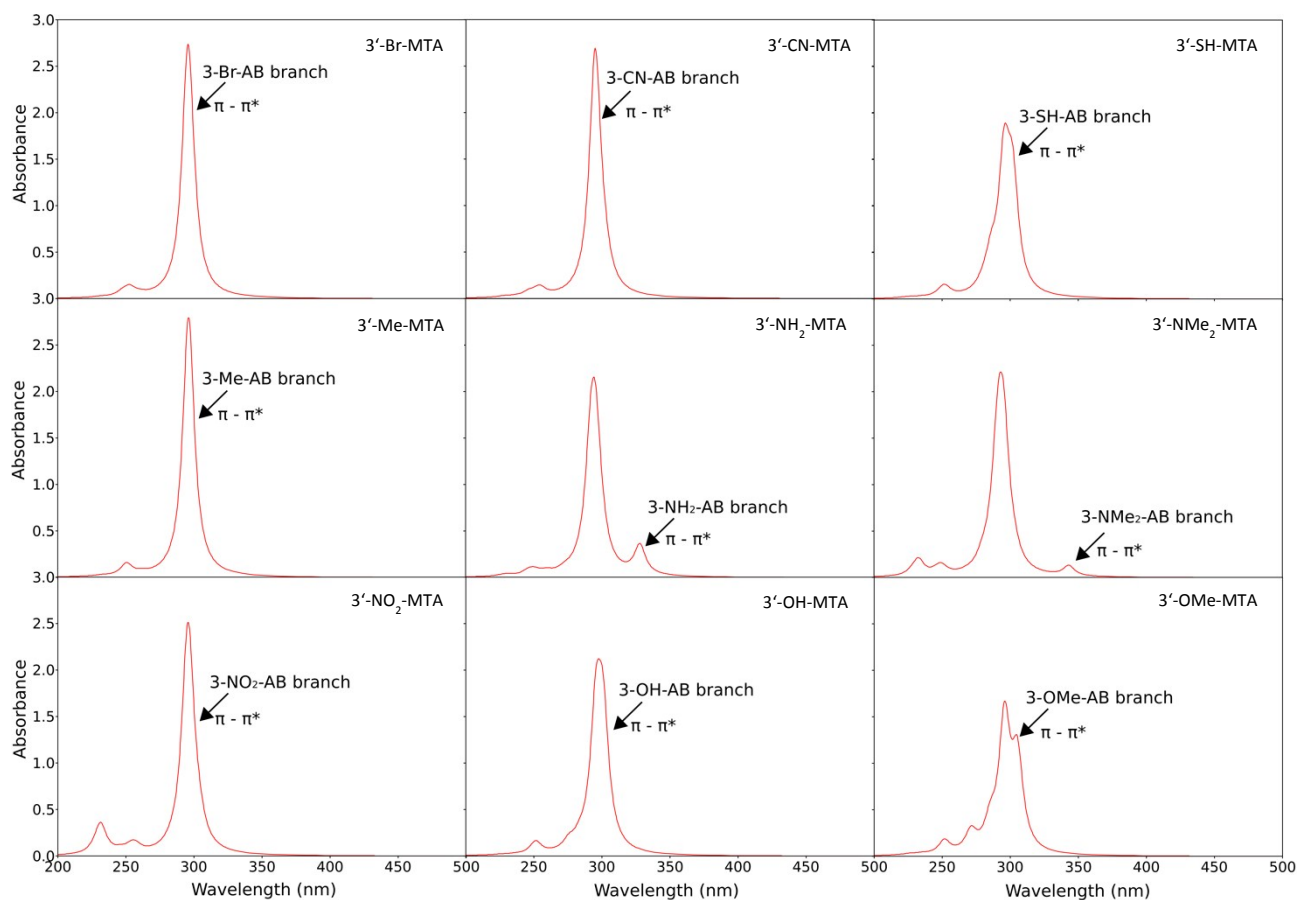


Figure S2: Simulated absorption spectra of single-branch substituted MTAs, which are all substituted at the 3' position, at the theoretical level of TDDFT/CAM-B3LYP. For the simulation of the spectra a full-width-at-half maximum of 10 nm has been used.

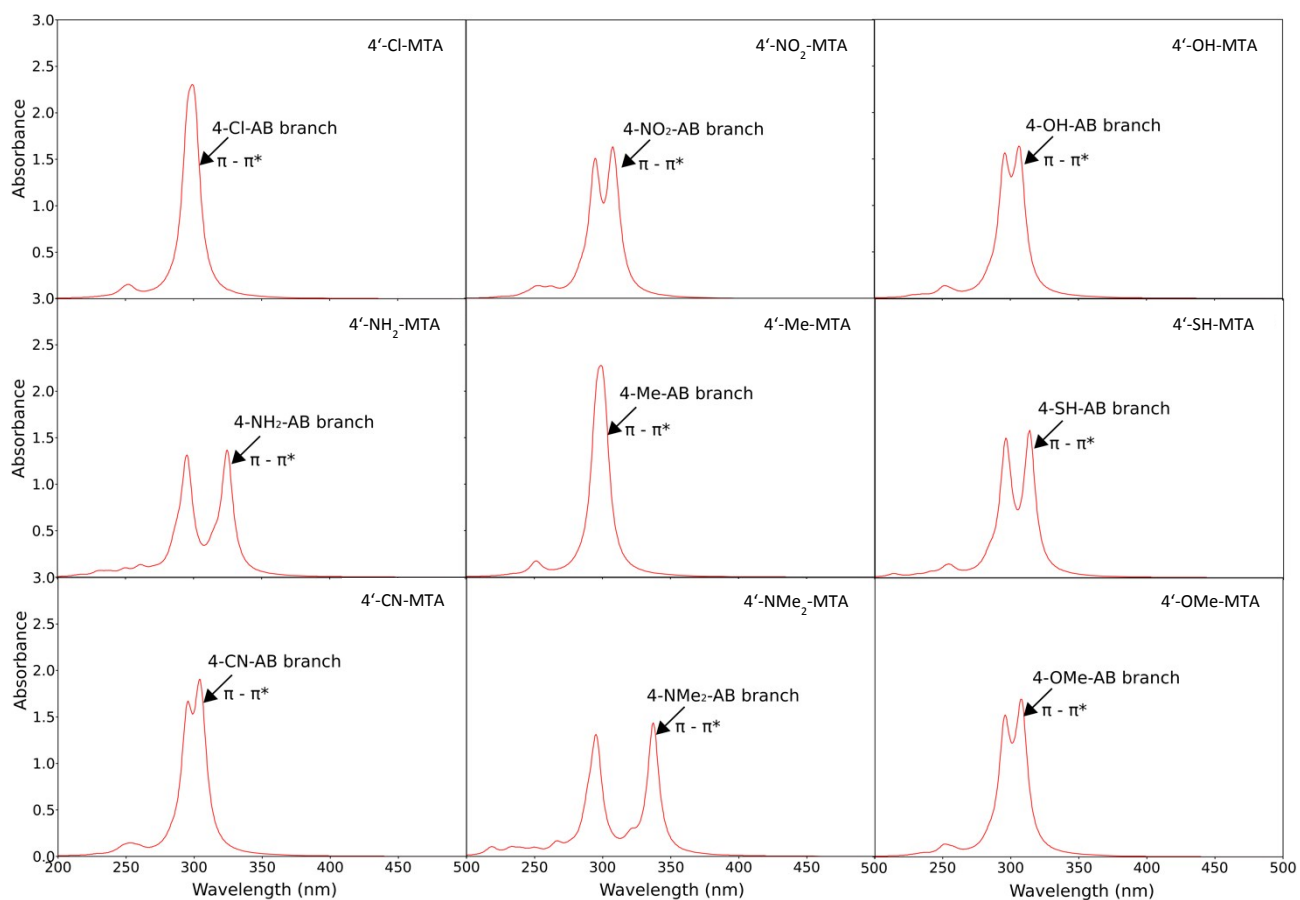


Figure S3: Simulated absorption spectra of single-branch substituted MTAs, which are all substituted at the 4' position, at the theoretical level of TDDFT/CAM-B3LYP. For the simulation of the spectra a full-width-at-half maximum of 10 nm has been used.

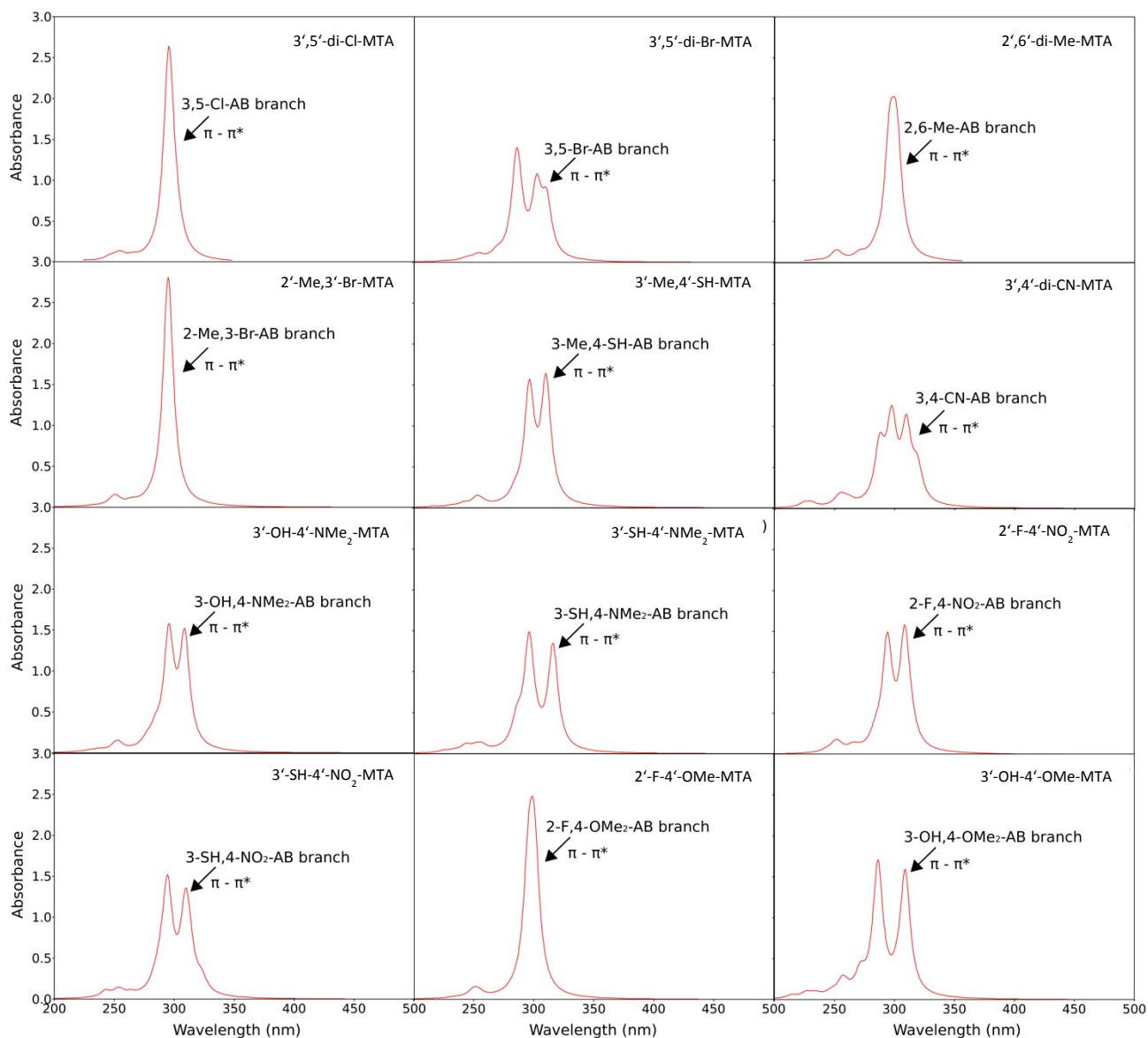


Figure S4: Simulated absorption spectra of single-branch substituted MTAs with two substituents at one terminal phenyl ring at the theoretical level of TDDFT/CAM-B3LYP. For the simulation of the spectra a full-width-at-half maximum of 10 nm has been used.

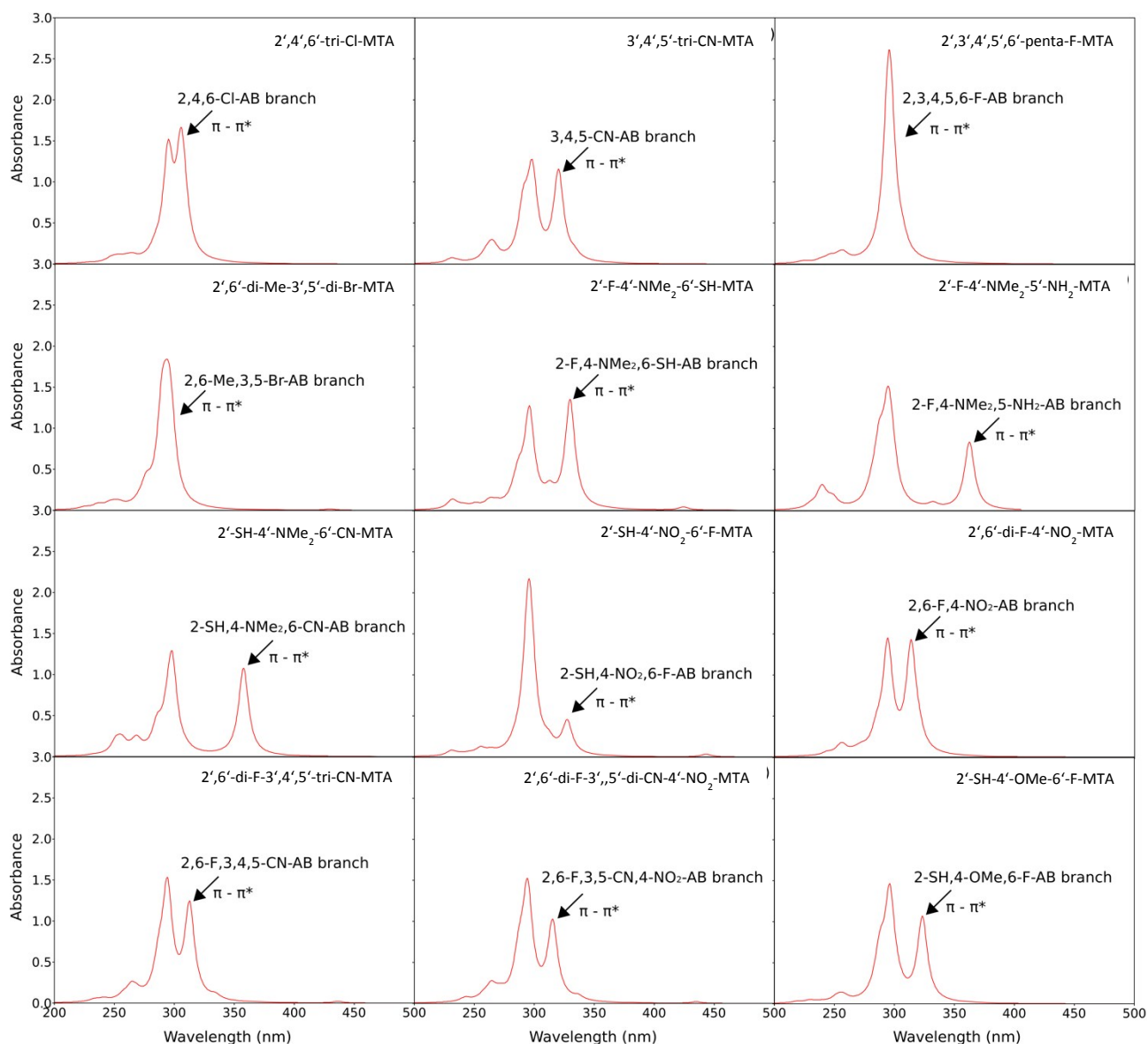


Figure S5: Simulated absorption spectra of single-branch substituted MTAs with multiple substituents at one terminal phenyl ring at the theoretical level of TDDFT/CAM-B3LYP. For the simulation of the spectra a full-width-at-half maximum of 10 nm has been used.

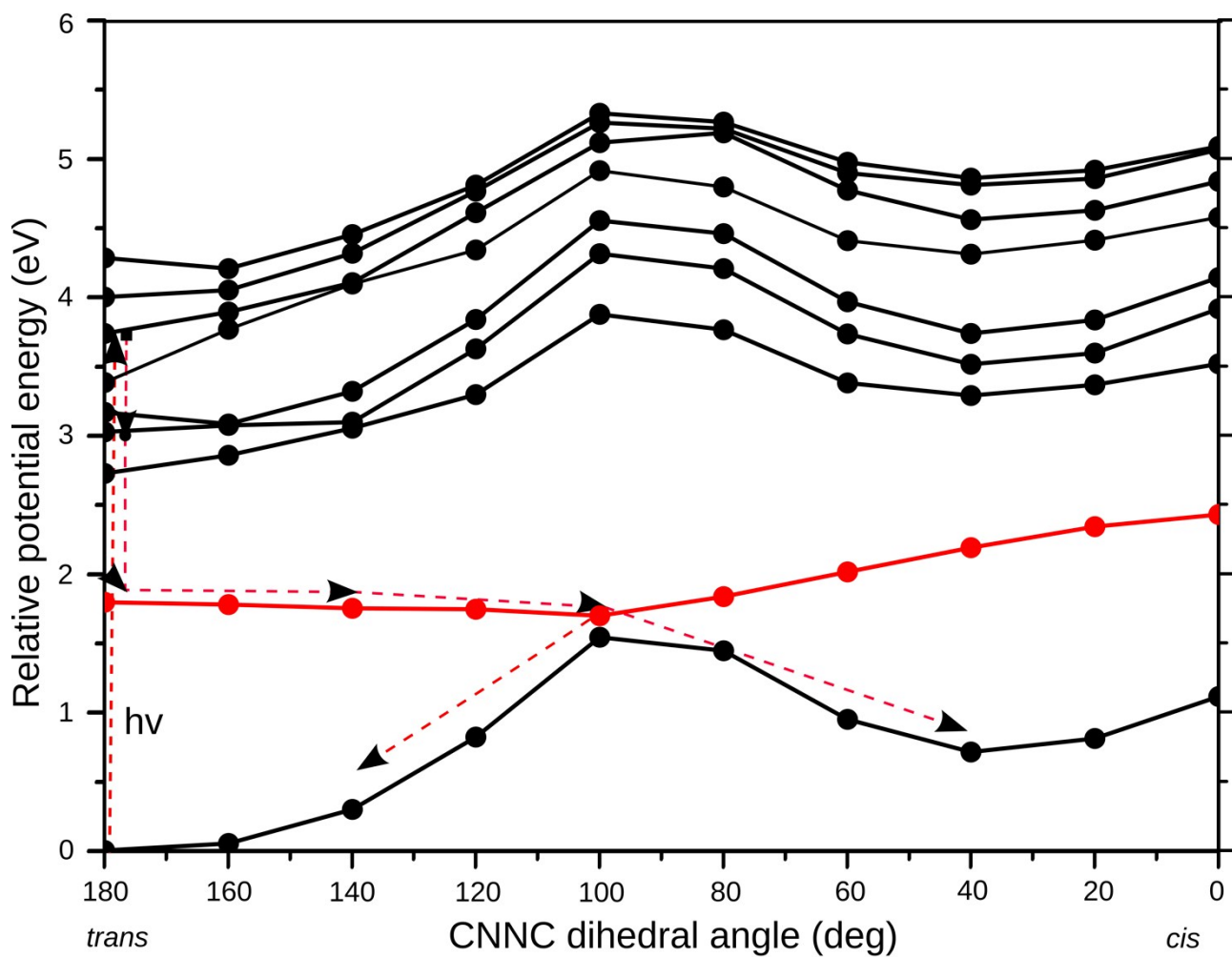


Figure S6: Relaxed scans of the potential energy surfaces along the isomerization pathway of the 4''-SH substituted AB branch of (2',4',6'-tri-CN-4''-SH)-MTA after unconstrained relaxation of S_6 . Initially, the excited S_6 $\pi\pi^*$ state decays into the S_1 $n\pi^*$ now localized at the 4''-SH substituted AB branch, which undergoes barrierless isomerization along the CNNC dihedral angle rotation.

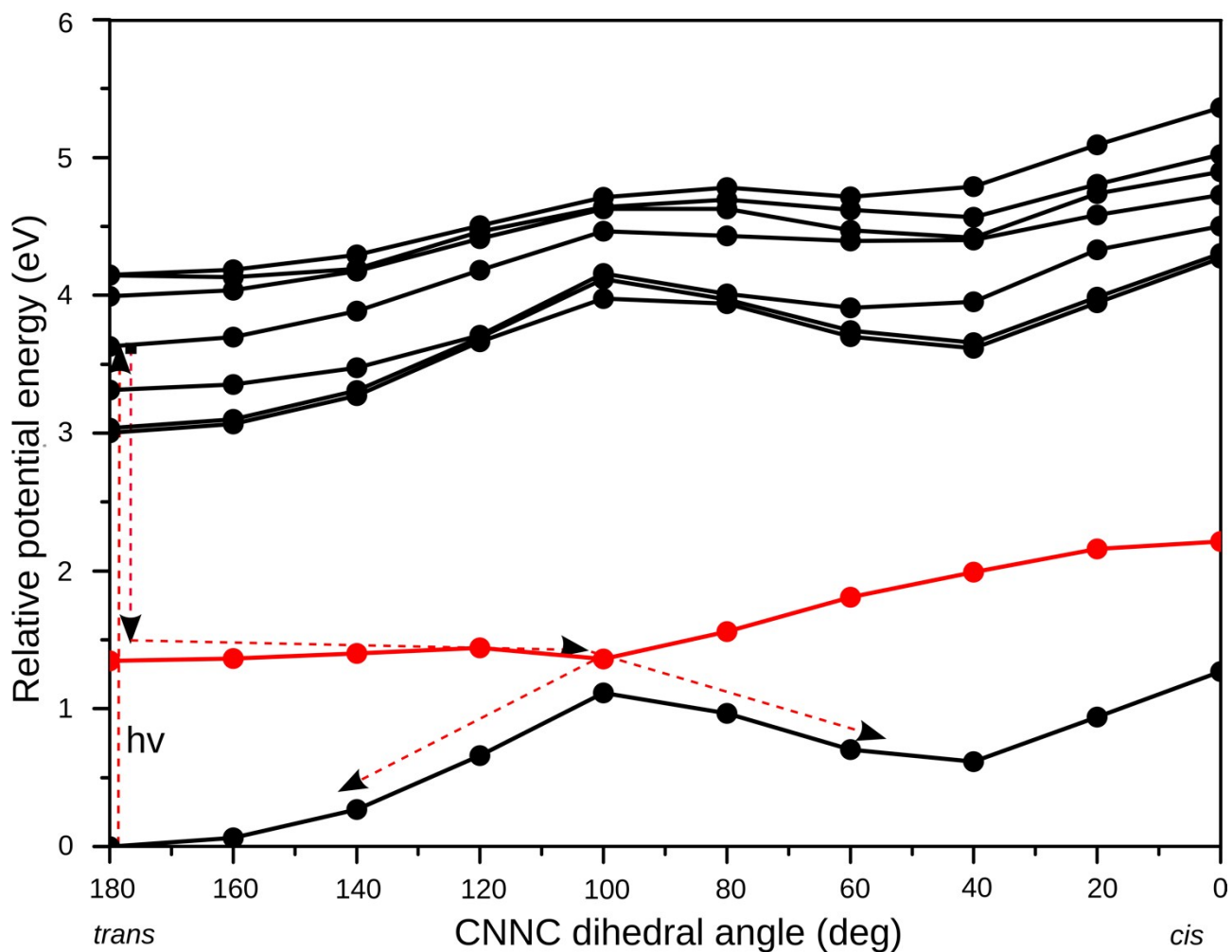


Figure S7: Relaxed scans of the potential energy surfaces along the isomerization pathway of the 2',4',6'-tri-CN substituted AB branch of (2',4',6'-tri-CN-4''-SH)-MTA after unconstrained relaxation of S_5 . Initially, the excited S_5 $\pi\pi^*$ state decays into the S_1 $n\pi^*$ state localized at the 2',4',6'-tri-CN substituted AB branch, which undergoes barrierless isomerization along the CNNC dihedral angle rotation.